Liquid Crystals
Publication details, including instructions for authors and subscription information:
http://www.informaworld.com/smpp/title~content=t713926090

Effects of the preparing condition of a polymer-stabilised liquid crystal with a smectic-A-chiral nematic phase transition on its properties

Guohui Pan[a]; Yubo Cao[b]; Renwei Guo[a]; Huicong Cheng[a]; Zhou Yang[a]; Jinbao Guo[a]; Xiaokai Liang[a]; Duowei Zhang[a]; Hui Cao[a]; Huai Yang[a]
[a] Department of Materials Physics and Chemistry, School of Materials Science and Engineering, University of Science and Technology Beijing, Beijing, P. R. China [b] Yawang Liquid Crystal Material Limited Company, Beijing, P. R. China

To cite this Article Pan, Guohui , Cao, Yubo , Guo, Renwei , Cheng, Huicong , Yang, Zhou , Guo, Jinbao , Liang, Xiaokai , Zhang, Duowei , Cao, Hui and Yang, Huai(2009) 'Effects of the preparing condition of a polymer-stabilised liquid crystal with a smectic-A-chiral nematic phase transition on its properties', Liquid Crystals, 36: 2, 165 — 172
To link to this Article: DOI: 10.1080/02678290902752132
URL: http://dx.doi.org/10.1080/02678290902752132

Liquid Crystals,
Vol. 36, No. 2, February 2009, 165–172

Taylor & Francis
Taylor & Francis Group

Effects of the preparing condition of a polymer-stabilised liquid crystal with a smectic-A–chiral nematic phase transition on its properties

Guohui Pan[a], Yubo Cao[b], Renwei Guo[a], Huicong Cheng[a], Zhou Yang[a], Jinbao Guo[a], Xiaokai Liang[a], Duowei Zhang[a], Hui Cao[a] and Huai Yang[a]*

[a]*Department of Materials Physics and Chemistry, School of Materials Science and Engineering, University of Science and Technology Beijing, Beijing 100083, P. R. China;* [b]*Yawang Liquid Crystal Material Limited Company, Beijing 100083, P. R. China*

(Received 19 November 2008; final form 15 January 2009)

A homeotropically-oriented polymer network stabilised liquid crystal (PSLC) film with a smectic-A (SmA)–chiral nematic (N*) phase transition was prepared. In the temperature range of the SmA phase, the liquid crystal (LC) molecules were homeotropically oriented and the film showed a transparent state. However, in the temperature range of the N* phase, the film showed a strong light scattering state due to the LC molecules adopting a focal conic alignment affected by the homeotropically-oriented polymer network. Moreover, the strong light scattering state of the N* phase could return to the transparent state when an electric field is applied on it. The focus of this study is on the effects of the preparing conditions of the PSLC film, including the curing temperature and the intensity of the ultraviolet (UV) irradiation on its thermo-optical and electro-optical properties.

Keywords: smectic-A phase; chiral nematic phase; homeotropic polymer network; electro-optical property; thermo-optical property

1. Introduction

The PSLCs are composites with a small amount of a crosslinked polymer dispersed in the anisotropic fluid. The general idea of PSLC is the stabilisation of the alignment of a low-molecular-mass liquid crystal (LC) by elastic interactions between the network and the LC (*1*). The polymer network is an important factor determining the thermo-electro-optical properties of the composites by stabilising the molecular orientation of LCs (*1–4*). PSLC films have provided a new field of LC science and technology (*5–19*), in which a desired macroscopic orientation of LC directors can be stabilised (*5–11*) or frozen (*12*, *13*) by the crosslinked network dispersed within the LC. For example, the three-dimensional cubic structure with lattice periods of several hundred nanometres in a blue phase, of which the temperature range is usually less than a few Kelvin, can be stabilised over a temperature range of more than 60 K (*9*). The planar molecular alignment of a N* phase can also be stabilised in a smectic-A (SmA) phase at a macroscopic level, and then the SmA phase has both the optical characteristics similar to those of a N* phase and the mechanical properties of a SmA phase (*10*). Moreover, the PSLC films with gradient pitch distribution and non-uniform pitch distribution as the brightness enhancement film of LC displays have also been prepared (*11–13*). Besides these, the PSLC films have many other potential applications, such as light shutters (*5–9*), E-papers (*10*), wide-band polarisers (*11–16*) and reflective LC displays (*17–19*).

The LC/polymer network system based on the phase transition of SmA–N* have been studied in recent years. This composite system is a promising candidate of LC display, E-paper and smart windows controlled by temperature. For example, the thermally-addressed and electrically-erasable LC display (TAEELCD) materials have been prepared and studied based on the composite system with the transition of SmA–N*; the light scattering state of SmA in the helical network formed in N* in the presence of the electrical field is used. Some regions are thermally addressed in the N* phase, and, on cooling, the addressed region in the SmA with the direction of LC molecules parallel to the substrate is transparent, the moment electric field is applied again, and the cell exhibits light scattering (*20*). The PSLC film with the property of transparency at lower temperatures and light scattering at higher temperatures is an excellent candidate for smart widows. The thermo-optical properties of PSLC film with a SmA–N* phase transition have been studied by Yang *et al.* (*21*). The PSLC film was prepared by ultraviolet (UV) radiation induced crosslinking between the molecules of a photo-polymerisable monomer in the homeotropically oriented SmA phase of the photo-polymerisable monomer/LC/photoinitiator mixture with a SmA–N* phase transition. When heating the PSLC film from the SmA to the N* phase, a sharp change occurs from a transparent to a light scattering state. On cooling from the N* to the SmA phase, the PSLC film can change from the

*Corresponding author. Email: yanghuai@mater.ustb.edu.cn

ISSN 0267-8292 print/ISSN 1366-5855 online

DOI: 10.1080/02678290902752132
http://www.informaworld.com

light scattering to the transparent state reversibly. However, the effects of the preparing conditions of the PSLC film on its properties have not been studied. In this study, we examined the effects of the preparing conditions of the PSLC film on its thermo-optical properties, as well as on the electro-optical properties of the N* phase of the PSLC film.

2. Experiments

2.1 Materials

The nematic LC, SLC-1717 (Shijiazhuang Yongsheng Huatsing Liquid Crystal Co., Ltd., Shijiazhuang City, Hebei Province, China), the chiral dopant, S811 (Merck Co., Ltd.) and the photo-initiator, 2, 2-dimethopxy-1, 2-diphenyl-ethanone (IRG651, TCI Co., Ltd.) were used. The SmA LC was prepared from cyanobiphenyls (8CB and nOCBs). The 8CB, the nOCBs and the photo-polymerisable LC diacrylate monomer, C6M, were synthesised according to the methods suggested by Gray *et al.* (*22*) and by Broer *et al.* (*23*), respectively. In Figure 1, we present the chemical structure and some physical parameters of these materials (the temperatures in Figure 1 are in Kelvin).

2.2 Preparation of samples

In order to induce a homeotropic orientation of LC molecules, the inner surfaces of indium tin oxide coated (ITO) glass cells were treated by N, N-dimethyl-N-octadecyl-3-aminopropyltrimethoxysilyl chloride (DMOAP) solution (0.1% by volume in water) (*24*) and 20 μm-thick poly (ethylene terephthalate) (PET) films were used as the cell spacers. To prepare the PSLC film, the samples of C6M/LCs/S811/photoinitiator mixtures (SmA 310.4 K, N* 335.8 K I) were filled into the cells by capillary action in their N* phases on 318.2 K. Then, the homeotropically oriented SmA phase of the samples cooled from the N* phase on 0.5 K min^{-1} were irradiated by the UV light (365.0 nm) for half an hour to induce crosslinking between the molecules of C6M in the samples.

(1) Photo-polymerizable LC monomer: C6M

Cr 356.4 N 388.8 I

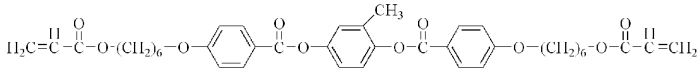

(2) Smectic-A LC: 8CB+nOCB

Mixture of LCs with positive dielectric anisotropy

Cr 269.1 SmA 327.5 N 329.6 I

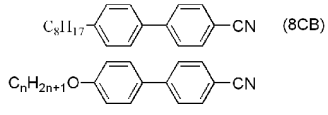

8CB: 60.0wt% n=10: 10.1wt% n=12: 6.7wt%

n=14: 7.2wt% n=16: 16.0wt%

(3) Nematic LC: SLC1717 (Yongsheng Huatsing Liquid Crystal Co., Ltd.)

Mixture of LCs with positive dielectric anisotropy

Cr 233.0 N 365.0 I

(4) Chiral Dopant: S811 (Merck Co., Ltd.)

Left-handed

Cr 320.2 I

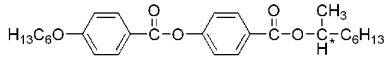

(5) Photoinitiator: 2, 2-dimethopxy-1, 2-diphenyl-ethanone (TCI Co., Ltd.)

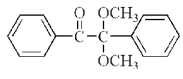

Figure 1. The chemical structures and some physical parameters of the materials used.

2.3 Measurements

The phase transition temperatures and the aggregation structure of the samples used were studied by differential scanning calorimetric (DSC) (Perkin-Elmer DSC 6) at a heating rate of 10.0 K min^{-1} and polarising optical microscopic (POM) (Olympus BX-51) at a heating rate of 1.0 K min^{-1}. The thermo-optical and electro-optical performances were investigated with a LC display parameters tester (LCT-5016C, Changchun Lianchen Instrument Co, Ltd., China). The polymer network for scanning electron microscopic (SEM) (Cambridge S360) observations were prepared in the following way. After UV irradiation of the cell for photo-polymerisation, the sealant material of the cell was removed to allow diffusion of hexane into the cell. After extracting the LC with hexane, the cell was dried *in vacuo* for a few hours. Then, the cell was opened with caution and the substrate, plus the polymer network, were coated with a thin gold layer to eliminate any electric charge problem for SEM study.

3. Results and discussion

Figure 2 shows the schematic representation of the preparation process of the expected PSLC film. At first, the C6M/LCs/S811/photoinitiator mixture was filled into the cell in the N* phase of the mixture as shown in Figure 2(a). On cooling the mixture to the SmA phase, this phase was homeotropically oriented as it was affected by the surface orientation agent. After the SmA phase was irradiated by UV light, the homeotropically-oriented polymer network from the crosslinking between the molecules of C6M was formed in the SmA phase, so the PSLC film was prepared as shown in Figure 2(b), exhibiting a transparent state. The film could return to the strong light scattering state (Figure 2(c)), accompanied by the texture changing from the homeotropic texture of SmA, to the focal conic state of N* when being heated above the SmA–N* phase transition temperature, due to both the anchoring effect of the polymer network and the orientation effect of the surface orientation agent. Strictly speaking, the long axes of LC molecules in the vicinity of the homeotropic polymer tended to remain perpendicular to the cell surfaces while the remaining LC molecules relaxed back to the spiral structure, that is, a focal conic texture was formed as the result of the competition between the intrinsic spiral structure and the constraining effect of the polymer network (*7*). The light scattering effect was attributed to the refractive indices mismatching between the small focal conic domains (*25*, *26*). On being cooled from the N* to the SmA phase, the film went back to the transparent state (Figure 2(b)). On the application of an electric field, the strong light scattering state was changed into the transparent state due to the LC molecules with positive anisotropy being homeotropically aligned by the applied electric field (Figure 2(d)).

The preparation conditions of different samples are listed in Table 1. All of the samples were prepared

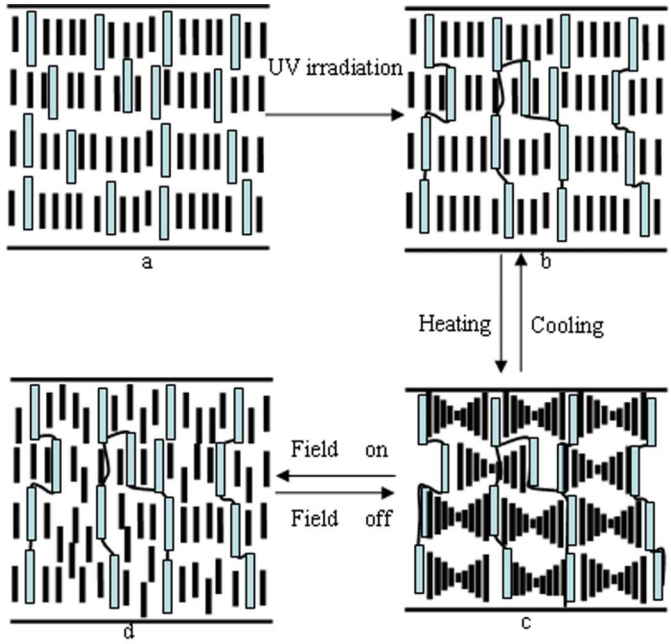

Figure 2. A schematic of the preparation scheme for the film.

Table 1. Preparation conditions for different samples.

Samples	Curing temperature (K)	Intensity of UV irradiation (mW cm^{-2})
A1	303.2	0.9
A2	303.2	1.2
A3	303.2	2.0
A4	303.2	2.9
A5	303.2	4.2
B1	281.2	1.2
B2	287.2	1.2
B3	297.2	1.2
B4	303.2	1.2

from the composition (C6M/LC (SmA LC/SLC1717) S811/wt% = 4.0/89.3 (69.7/19.6)/6.7). The effect of the intensity of UV irradiation on thermo-optical and electro-optical properties of the PSLC film is studied from sample A1 to A5. The influence of the curing temperature on the thermo-optical and electro-optical properties is investigated from sample B1 to B4.

SEM photographs of the morphology of the homeotropically-oriented polymer network are shown in Figure 3. The monomer used was listed in Figure 1, the constituents of which included a mesogenic core, reactive endgroups and flexible alkyl spacer chains between the core and the endgroups (*7*, *27*). The acrylate functional groups are attached to both sides of the mesogenic core by a flexible alkyl chain, the mesogenic core is aligned with the individual monomer molecules with the local liquid crystalline order, while the flexible alkyl chains allowed adjacent cores to align themselves parallel to one another during polymerisation (*28*). As mentioned above, the monomer was polymerised in homeotropic SmA; during photo-polymerisation, the order of the SmA phase was templated by the formed polymer network, so it was reasonable to say that the polymer network should be oriented homeotropically in the cell. Figure 3 shows the morphology of the polymer network from which the fibrous polymer network perpendicular to the substrate was observed. The SEM photographs were taken while the angle between the observing direction and the normal cell substrate was about 90.0° and 0.0°, respectively. The polymer network was composed of polymer strands oriented along the direction of the director. The smooth fibrous morphology of the polymer network was attributed to the good solubility of the monomer in the LCs. Generally, below the solubility limit, undergoing a radical chain polymerisation leads to a smooth polymer network. The behaviour may be understood in the context of the Flory-Huggins model of polymer solubility, which is the primary factor determining the network morphology (*29*, *30*).

Figure 4 shows SEM photographs of the homeotropically-oriented polymer network for samples A1–A5. It can be seen from Figure 4 that the size of the meshes of the polymer network decreased in sequence. Since the mechanism of the photo-polymerisation of the LC monomer is radical polymerisation, it is easy to understand that increasing the intensity of UV irradiation, from which more free radicals are created, leads to denser polymer networks with smaller voids.

Figure 5 shows the temperature dependence of the transmittances for different intensity of UV irradiation prepared from samples A1–A5. It can be seen from Figure 5 that samples A1–A5 all exhibited a quick switch between the transparent state and the strong light scattering state, which was because the SmA–N* phase transition is a very weak first order or second order transition (*31*, *32*). The transmittance of the transparent state in the range of 80.0–90.0% showed an excellent light transmitting property, while the transmittance of the light scattering state of the samples was less than 1.0%, showing a good light blocking property. The loss of light intensity in the transparent state was mainly due to the reflections

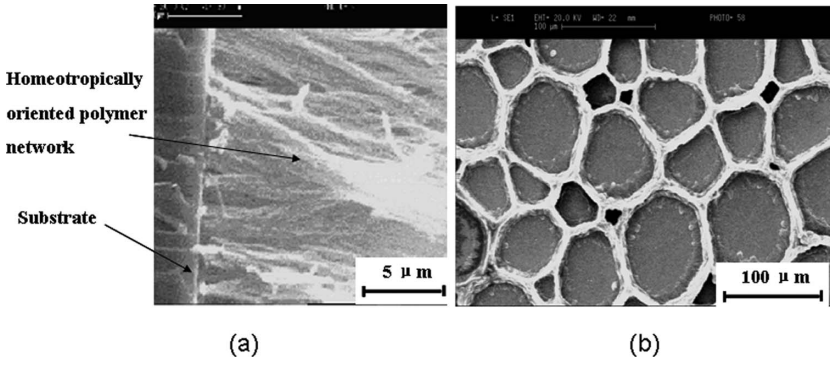

Figure 3. SEM photographs of the homeotropically-oriented polymer network observed with angles between the observing direction and the normal substrate surface being about (a) 90.0°, (b) 0.0°.

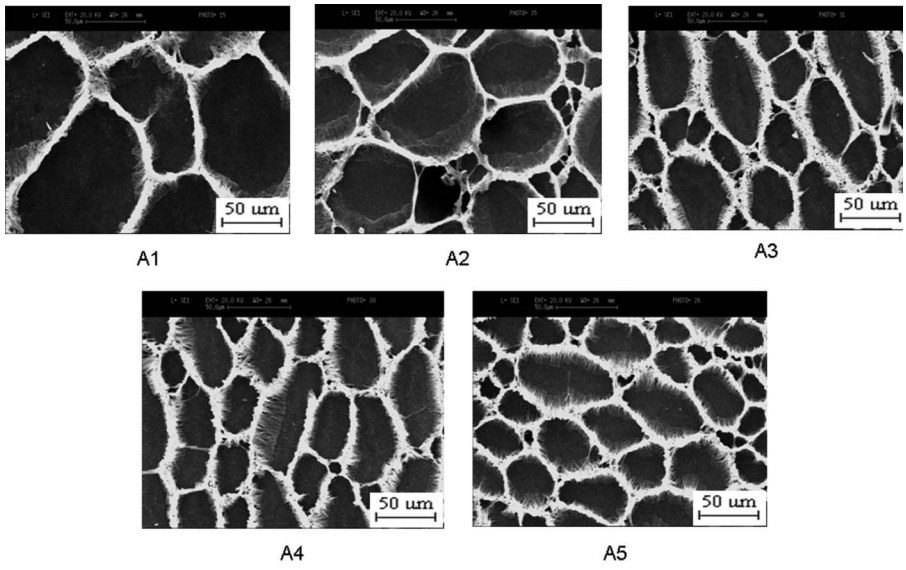

Figure 4. SEM photographs of the homeotropically oriented polymer network for samples A1–A5.

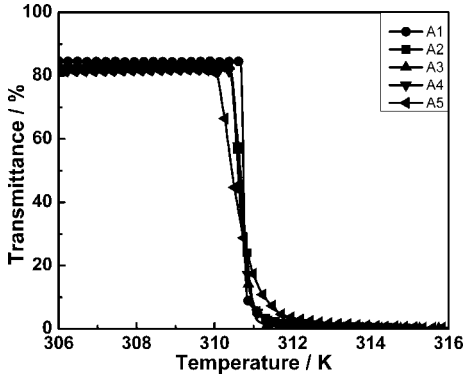

Figure 5. Plot of the temperature dependence of transmittance for samples A1–A5.

from the glass-air interfaces (*7*). However, the speed of transition from the transparent state to the light scattering state decreased with increased intensity of the UV irradiation, because the homeotropically-oriented polymer network became more and more dense as the intensity of the UV irradiation increased. Hence, the switching process from the transparent state to the light scattering state was affected by the homeotropically-oriented polymer network.

The intensity of the UV irradiation dependence of the electro-optical properties for the composites prepared from samples A1–A5 is shown in Figure 6. A change from the focal conic texture (Figure 2(c)) to the homeotropic texture (Figure 2(d)) was realised when the electric field was applied to the N* phase. This change was realised when the LC molecules had a positive dielectric anisotropy and an electric field higher than the critical value $EC = \frac{\pi^2}{po}\sqrt{\frac{K_{22}}{\varepsilon o \Delta\varepsilon}}$ was applied (*33*, *34*). Here, the measured electro-optical parameters included the threshold voltage (V_{th}), the saturation voltage (V_{sat}), the field-on response time (T_{on}) and the field-off response time (T_{off}). The threshold voltage (V_{th}) and the saturation voltage (V_{sat}) are defined as the voltage required for the transmittance reaching 10% and 90%, respectively. The T_{on} and T_{off} are defined as the time for the transmittance to go from 10% to 90% (or 90% to 10%) of the total change between the on and off states. The contrast ratio is defined as the larger of the two transmittance values divided by the smaller of the two values. The intensity of the UV irradiation dependence of the V_{th} and the V_{sat} is shown in Figure 6(a). It can be found that both the V_{th} and the V_{sat} decreased with increased intensity of UV irradiation, which was due to the elastic interaction between the polymer network and the LC molecules getting stronger, owing to a more and more dense polymer network from the increasing intensity of UV irradiation, so less energy was needed to complete the unwind process. Figure 6(b) shows the intensity of the UV irradiation dependence of the T_{on} and the T_{off}. The T_{on} decreased with increased intensity of UV irradiation, whereas T_{off} increased with increased intensity of UV irradiation, which was because less time was needed for the LC molecules to unwind the helical structure, while more time was needed for the LC molecules to go back to the original helical structure with increased intensity of UV irradiation, since the elastic interaction between the LC molecules and the polymer network was getting stronger with the increased intensity of UV irradiation. The intensity of the UV irradiation dependence of the contrast ratio is shown in Figure 6(c). The contrast ratio

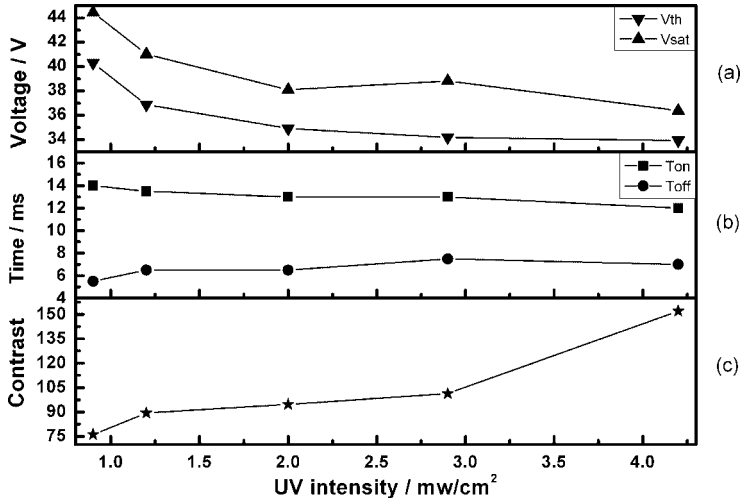

Figure 6. Plot of the intensity of the UV irradiation dependences of (a) V_{th} and V_{sat}, (b) T_{on} and T_{off} and (c) contrast ratio for samples A1–A5.

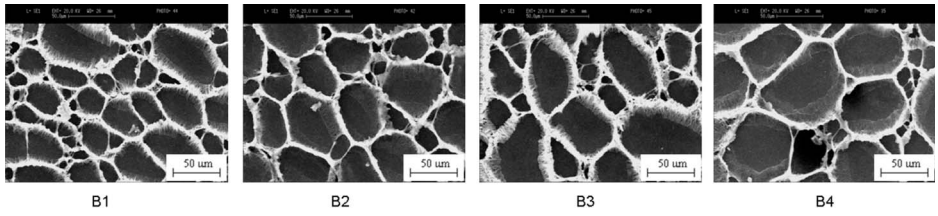

Figure 7. SEM photographs of the homeotropically-oriented polymer network for samples B1–B4.

increased as the intensity of the UV irradiation increased. This was because the increasingly dense polymer network from the increased intensity of UV irradiation could lead to a more scattering domain.

Figure 7 shows the SEM photographs of the homeotropically-oriented polymer network for samples B1–B4. It can be found that the size of the meshes of the polymer network increased with increased curing temperature. It is known that the viscosity of the LC system in the samples decreased with an increased curing temperature; the diffusion speed of the molecules is less limited, so the size of the meshes of the polymer network increased with the increased curing temperature. This can be further explained as follows. The formation of the polymer network results from the competition process between nucleation and the growth of the initial nucleus. At lower temperatures, since the diffusion rate is proportional to the activation energy, the activity of the prepolymer is slow, that is, the growth speed of the initial nucleus is slow. Since the speed of the nucleation of the polymer network is hardly affected by curing temperature, which was mainly determined by UV irradiation intensity, the density of the polymer network is relatively high. At higher temperatures, the movement of the prepolymer becomes faster, that is, the growth speed of the initial nucleus becomes faster, while the variation of curing temperature has almost no effect on the speed of nucleation of the polymer network. Hence, the density of the polymer network decreased.

Figure 8 shows the temperature dependence of the transmittances for different curing temperatures prepared from samples B1–B4. It could be known that the

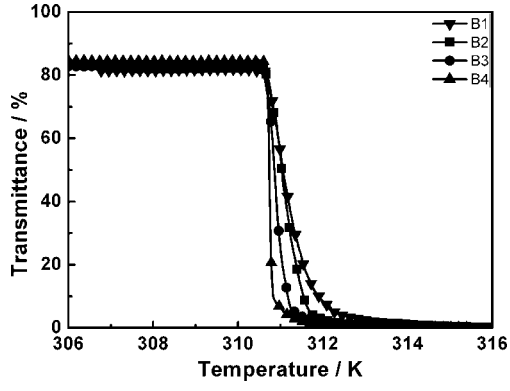

Figure 8. Plot of the temperature dependence of transmittance for samples B1–B4.

speed of the transition of samples B1–B4 from the transparent state to the light scattering state increased with increased curing temperature. This was because the size of the meshes of the homeotropically-oriented polymer network became increasingly large with the increased curing temperature mentioned above, then the switching process from the transparent state to the light scattering state was influenced by the polymer network with different meshes.

The curing temperature dependence of the electro-optical properties for the composites prepared from samples B1–B4 is shown in Figure 9. Figure 9(a) shows the curing temperature dependence of the voltage. The V_{th} and the V_{sat} both increased with increased curing temperature. Since the elastic interaction between the polymer network and LC molecules became weaker, owing to the greater number of large voids in the polymer network from the increased curing temperature, more energy was needed to realise the unwind process. Figure 9(b) shows the curing temperature dependence of the T_{on} and the T_{off}. The T_{on} increased with increased curing temperature, whereas the T_{off} slightly decreased as the curing temperature increased. Since the elastic interaction between the LC molecules and the polymer network was getting weaker with the increased curing temperature as mentioned above, it takes more time for the LC molecules to unwind the helical structure, while less time was needed for the LC molecules to go back to the original helical structure. The curing temperature dependence of the contrast ratio is shown in Figure 9(c). The contrast ratio decreased with increased curing temperature, which was because fewer scattering domains were obtained, owing to the greater number of large voids in the polymer network from the increased curing temperature.

Figure 10 shows the photograph of the cell. When the environmental temperature became higher than the SmA–N* phase transition temperature, the cell changed from the transparent state, as shown in Figure 10(a), into the light scattering state as shown in Figure 10(b), and *vice versa*.

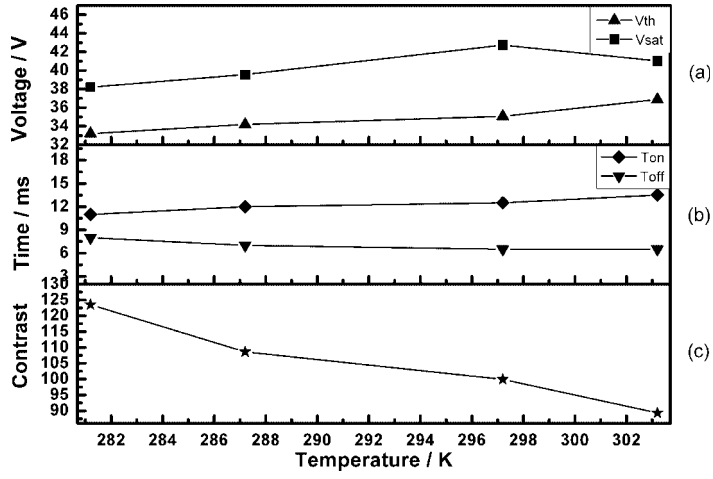

Figure 9. Plot of the intensity of the curing temperature dependences of (a) V_{th} and V_{sat}, (b) T_{on} and T_{off} and (c) contrast ratio for samples B1–B4.

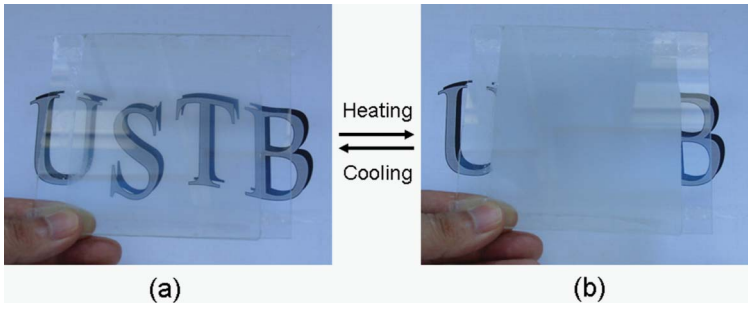

Figure 10. Photographs of the cell switching between the transparent state and the light scattering state.

4. Conclusions

In this study, the polymer network/LC/chiral dopant composite film prepared from the photo-polymerisation of a LC monomer/LC/chiral dopant/photoinitiator mixture was prepared and the effects of the preparation conditions of the film on its thermo-optical and electro-optical properties were studied. The results indicate that increased intensity of UV irradiation led to a denser polymer network with smaller voids, whereas a polymer network with a greater number of large voids is obtained with increased curing temperature. The speed of the transition from the transparent state to the light scattering state is slightly influenced by the polymer network. The switching characteristics between the light scattering state and the transparent state of the N* phase were also studied. Both the V_{th} and the V_{sat} decreased and increased with increased intensity of UV irradiation and the curing temperature, respectively. The T_{on} decreased and increased with increased intensity of UV irradiation and the curing temperature, respectively, while T_{off} had the opposite changing tendency. It is believed that the film has great potential for alarm devices for overheating or other thermo-electrical sensors.

Acknowledgements

Financial support from the Hi-tech Research and Development Program of China (Grant No. 2006AA03Z108), Program of Beijing Municipal Science and Technology (Grant No. Y045004040121) and Projects of Chinese National Science and Technology Tackling Key Problems (Grant No. 2006 BAI03A09) are gratefully acknowledged.

References

(1) Dierking I.; *Adv. Mater.* **2000**, *12*, 167–181.
(2) Binet C.; Mitov M.; Mauzac M. *J Appl Phys.*, **2001**, *90*, 1730–1734.
(3) Mitov M.; Nouvet E.; Dessaud N. *Eur Phys J E.*, **2004**, *15*, 413–419.
(4) Liu J.H.; Hung H.J.; Wu D.S.; Hong S.M.; Fu A.Y. *Appl Polym Sci.* **2005**, *98*, 88–95.
(5) Crawford G.P.; Zumer S. *Liquid Crystals in Complex Geometries*; Taylor & Francis: London, 1996; pp 124–126.
(6) Broer D.J. *Radiation Curing in Polymer Science and Technology*; Elsevier Science: London, 1993; pp 383–443.
(7) Yang D.K.; Chien L.C.; Doane J.W. *Appl. Phys. Lett.* **1992**, *60*, 3102–3104.
(8) Yang H.; Mishima K.; Matsuyama K.; Hayashi K.I.; Kikuchi H.; Kajiyama T. *Appl. Phys. Lett*. **2003**, *82*, 2407–2409.
(9) Kikuchi H.; Yokota M.; Hisakado Y.; Yang H.; Kajiyama T. *Nature Mater.* **2002**, *1*, 64–68.
(10) Yang H.; Kikuchi H.; Kajiyama T. *Chem. Lett.* **2003**, *32*, 256–257.
(11) Hikmet R.A.M.; Kemperman H. *Liq. Cryst.* **1999**, *26*, 1645–1653.
(12) Hikmet R.A.M.; Kemperman H. *Nature* **1998**, *392*, 476–479.
(13) Bian Z.Y.; Li K.; Huang W.; Cao H.; Yang H. *Appl. Phys. Lett.* **2007**, *91*, 201908–201910.
(14) Mitov M.; Dessaud N. *Nature Mater*. **2006**, *5*, 361–364.
(15) Relaix S.; Bourgerette C.; Mitov M. *Appl. Phys. Lett.* **2006**, *89*, 251907–251909.
(16) Ren H.W.; Wu S.T. *J. Appl. Phys.* **2002**, *92*, 797–800.
(17) Wu S.T.; Yang D.K. *Reflective Liquid Crystal Display*; Wiley: Singapore, 2001; pp 197–198.
(18) Chien L.C.; Cho J.; Leroux N. *Proc. SPIE.* **1998**, *129*, 3421–3427.
(19) Lu S.Y.; Chien L.C. *Appl. Phys. Lett.* **2007**, *91*, 131119–131121.
(20) Yang H.; Kikuchi H.; Kajiyama T. *Mol. Cryst. Liq. Cryst.* **2002**, *381,* 85–99.
(21) Yang H.; Kikuchi H.; Kajiyama T. *Liq. Cryst.* **2000**, *27*, 1695–1699.
(22) Gray G.W.; Harrison K.J.; Nash J.A. *Electron. Lett.* **1973**, *9*, 130–131.
(23) Broer D.J.; Boven J.; Mol G.N. *Makromol. Chem.* **1989**, *190*, 2255–2268.
(24) Kahn F.J. *Appl. Phys. Lett.* **1973**, *22*, 386–388.
(25) Mochizuki A. *Proc. SID* **1990**, *31*, 155–120.
(26) Wysocki J.; Adams J.; Haas W. *Liquid Crystals*, Brown G.H., Eds.; Wiley: New York, 1968; pp 135–136.
(27) Fung Y.K.; Yang D.K.; Ying S.; Chien L.C.; Zumer S.; Doane J.W. *Liq. Cryst.* **1995**, *19*, 797–801.
(28) Dierking I.; Kosbar L.L.; Lowe A.C.; Held G.A. *Appl Phys. Lett.* **1997**, *71*, 2454–2456.
(29) Rajaram C.V.; Hudson S.D.; Chien L.C. *Chem. Mater.* **1995**, *7*, 2300–2308.
(30) Muzic D.S.; Rajaram C.V.; Chien L.C.; Hudson S.D. *Polym. Adv. Technol.* **1996**, *7*, 737–745.
(31) de Gennes P.G. *Solid St. Commun.* **1972**, *10*, 753–756.
(32) Lubensky T.C.; Renn S.R. *Phys. Rev. A* **1990**, *41*, 4392–4401.
(33) Chandrasekhar S. *Liquid Crystals*; Cambridge University Press: New York, 1992, pp 135–136.
(34) Meyer R.B. *Appl. Phys. Lett.* **1969**, *14*, 208–209.